Electronic Supplementary Material

Direct pyrolysis to convert biomass to versatile 3D carbon nanotubes/mesoporous carbon architecture: conversion mechanism and electrochemical performance

Chenxi Xu[1]*, Shunli Li[1]*, Zhaohui Hou[2], Liming Yang[3], Wenbin Fu[4], Fujia Wang[4], Yafei Kuang[1], Haihui Zhou **(✉)**[1], Liang Chen **(✉)**[2]

1 College of Chemistry and Chemical Engineering, Hunan University, Changsha 410082, China

2 Key Laboratory of Hunan Province for Advanced Carbon-based Functional Materials, School of Chemistry and Chemical Engineering, Hunan Institute of Science and Technology, Yueyang 414006, China

3 Key Laboratory of Jiangxi Province for Persistent Pollutants Control and Resources Recycle, Nanchang Hangkong University, Nanchang 330063, China

4 School of Materials Science and Engineering, Georgia Institute of Technology, Atlanta 30332, United States

E-mails: clvilance@163.com (Chen L); haihuizh@163.com (Zhou H)

* These authors contributed equally to this work.

Table of Contents

Fig. S5 SEM images of CNTs/MC–C (10/3/100) (a), CNTs/MC–G (10/3/100) (b), CNTs/MC–S (10/3/100) (c) and CNTs/MC–Y (0/3/100) (d)

Fig. S6 SEM images of CNTs/MC–C (10/0/100) (a), CNTs/MC–G (10/1.5/100) (b), CNTs/MC–S (10/6/100) (c), CNTs/MC–Co (10/3/100) (d) and CNTs/MC–Ni (10/3/100) (e)

Fig. S7 SEM images of CNTs/MC–Y (10/3/0) (a), CNTs/MC–Y (10/3/10) (b) and CNTs/MC–Y (10/3/500) (c)

Fig. S8 SEM images of CNTs/MC–600 (10/3/100), CNTs/MC–700 (10/3/100) and CNTs/MC–900 (10/3/100)

Fig. S9 Long–term cycling performance of CNTs/MC–Y (10/3/100) electrode at the current density of 0.5 A g^{-1}

Fig. S10 Equivalent circuit model for the EIS plots

Fig. S11 CV curves on CNTs/MC–Y (10/3/100) electrode in N_2 and O_2 saturated 0.1 M KOH electrolyte

Fig. S12 LSV curves on CNTs (a) and MC (b) electrodes at different rotation speeds

Fig. S13 (a) The relative current density *vs.* time plots on CNTs/MC–Y (10/3/100) and commercial Pt/C electrodes at 0.67 V for 20000 s in O_2 saturated 0.1 M KOH electrolyte; (b) The relative current density *vs.* time plots on CNTs/MC–Y (10/3/100) and commercial Pt/C electrodes at 0.67 V in O_2 saturated 0.1 M KOH electrolyte before and after adding 3 M methanol

Table S1 The specific BET result of different samples

Table S2 Comparison of the ORR performance of previously reported

biomass–derived carbon catalysts with that of our work

1.1 Material characterizations

Scanning electron microscope (SEM, Hitachi SU 8010) and transmission electron microscope (TEM, JEM–2100F) were employed to check the micromorphology of our prepared samples. X–ray diffraction (XRD, Panalytical XPert PRO Alpha–1) and Raman spectroscopy (Labram–010) were exploited to measure the phase structure and defect nature of samples. X–ray photoelectron spectroscopy (XPS) was performed on a K–Alpha system (Thermo Scientific) to detect the chemical composition of samples. The Brunauer–Emmett–Teller analysis was conducted by TriStar II 3020 surface area and porosity measurement system.

1.2 Electrochemical measurements

1.2.1 ORR performance

The ORR performance was measured by three–electrode system on an electrochemical workstation (Gamry, INTERFACE 1010E) equipped with a rotating disk electrode (RDE 710, Φ=5 mm). The working electrode was prepared as follows. 10 μL of 2 mg mL^{-1} dispersed sample ink was transferred onto the polished RDE, and then a certain amount of Nafion solution was dropped onto the RDE to attain the working electrode. A Pt filament and Ag/AgCl electrode filled with saturated KCl were used as counter electrode and reference electrode, respectively. 0.1 M KOH aqueous solution was utilized as electrolyte. All potentials were converted to reversible hydrogen electrode (RHE) by the equation: $E_{RHE}=E_{Ag/AgCl}$ + 0.97 V. Before

every test, the electrolyte was bubbled with N_2 or O_2 for at least half an hour. Cyclic voltammetry (CV) was executed in N_2 or O_2 saturated 0.1 M KOH electrolyte between 1.17 V and –0.03 V. Linear sweep voltammetry (LSV) was tested at 10 mV s^{-1} at different rotation speeds from 400 to 1600 rpm. The ORR kinetic parameters can be calculated by Koutechy–Levich (K–L) equation:

$$\frac{1}{J} = \frac{1}{0.62nFC_0D_0^{2/3}\nu^{-1/6}\omega^{1/2}} + \frac{1}{J_k}$$

Where J represents tested current density, J_K is kinetic current density. n is electron transfer number, F refers to Faraday constant (96485 C mol^{-1}), C_0 is O_2 bulk concentration (1.2×10^{-3} M), D_0 stands for oxygen diffusion coefficient (1.9×10^{-5} cm^2 s^{-1}), ν is electrolyte kinetic viscosity (0.01 cm^2 s^{-1}) and ω is disk angular velocity.

1.2.2 LIBs performance

The battery performance was conducted by using two–electrode coin cells (CR 2025). The electrodes were prepared by blending active material, acetylene black, and polyvinylidene difluoride (PVDF) binder in a mass ratio of 8:1:1 in N–methyl–2–pyrrolidone (NMP). After stirring for several hours, the obtained homogeneous slurry was casted onto copper foil followed by vacuum drying and punching into circles with diameter of 15 mm. Lithium foil and microporous polypropylene membrane were used as counter electrode and separator, respectively. A mixed solvent consisting of dimethyl carbonate/ethyl methyl carbonate/ethylene carbonate (*v*/*v*/*v*=1:1:1) and 1 M $LiPF_6$ constituted the electrolyte. Cells assembly was manipulated in an argon–filled glovebox (both water and oxygen contents were limited to lower than 0.1 ppm). The galvanostatic charge/discharge curves were tested

on a Land battery system (CT 2001A). Cyclic voltammetry (CV) and electrochemical impedance spectroscopy (EIS) were measured on the electrochemical workstation (Gamry). EIS plots were recorded within the frequency range from 0.01 to 100 kHz. CV was tested at a scan rate of 0.5 mV s^{-1} from 0.005 to 3.0 V.

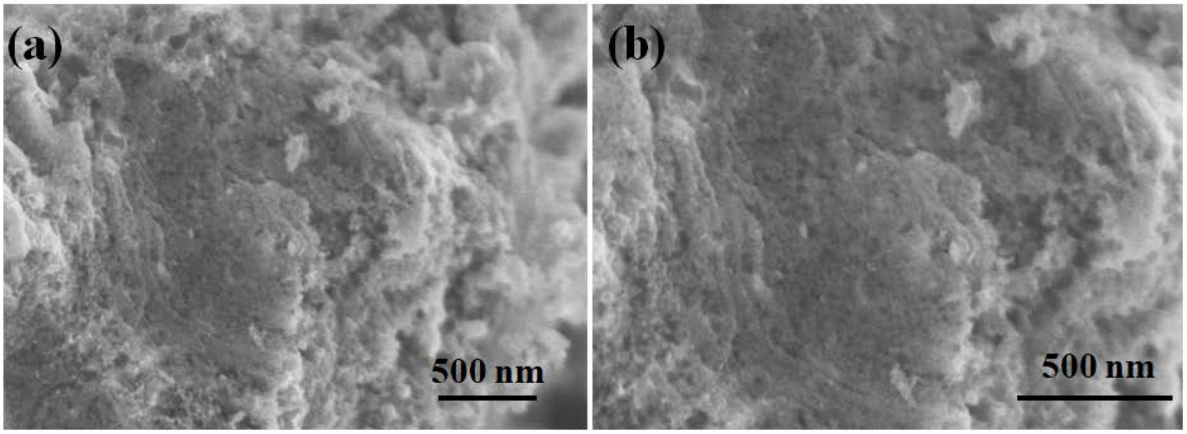

Fig. S1 SEM images of MC under different magnifications

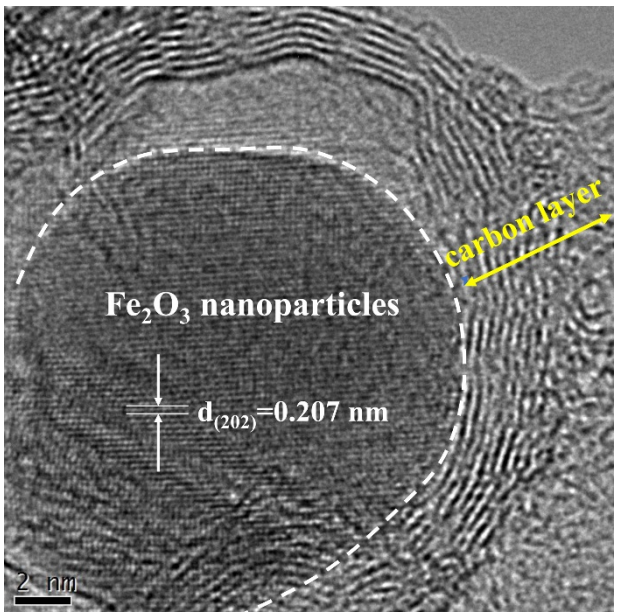

Fig. S2 HRTEM image of CNTs/MC–Y (10/3/100) hybrid

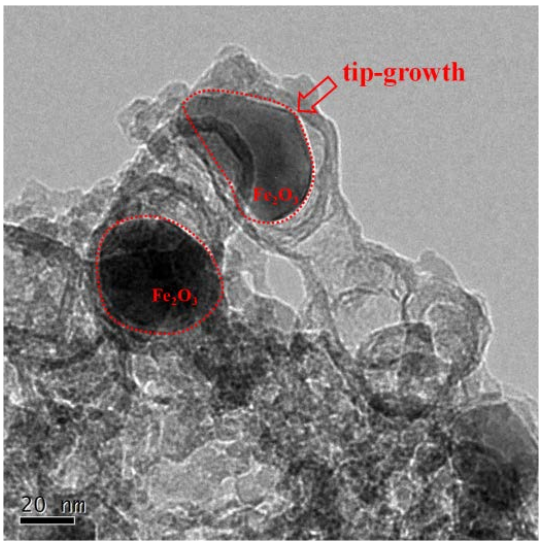

Fig. S3 Magnified TEM image of CNTs/MC–Y (10/3/100)

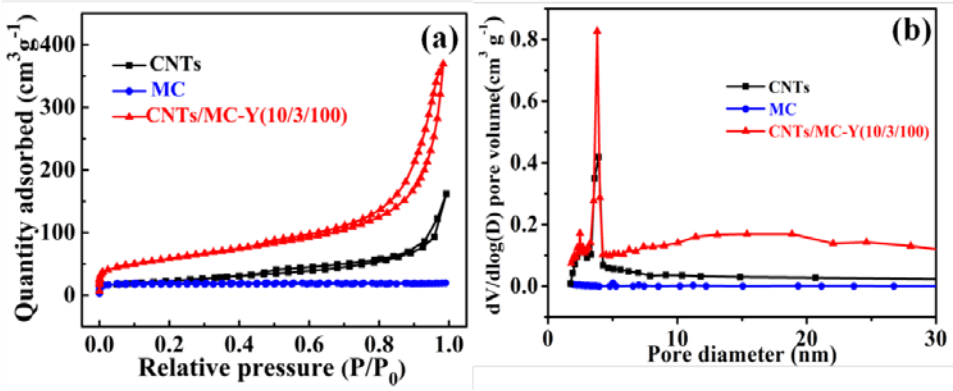

Fig. S4 N_2 adsorption/desorption isothermal curves and pore size distribution curves of CNTs, MC and CNTs/MC–Y (10/3/100) hybrid

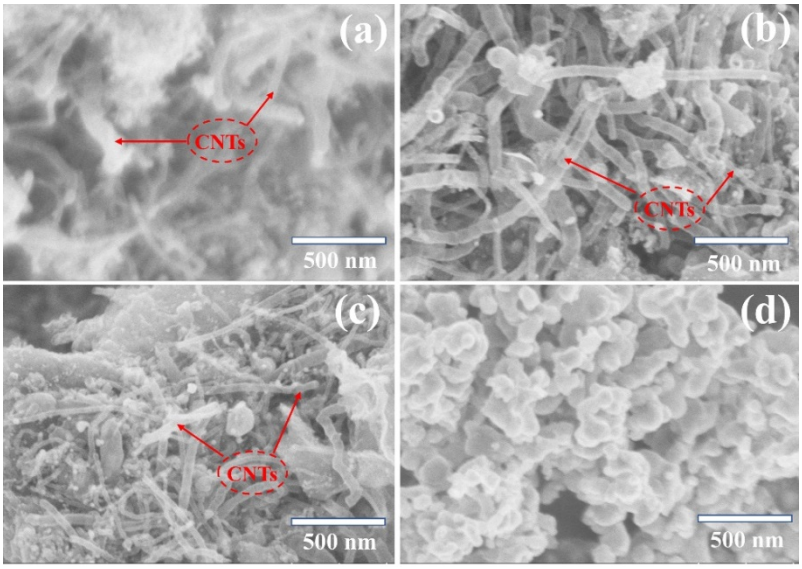

Fig. S5 SEM images of CNTs/MC–C (10/3/100) (a), CNTs/MC–G (10/3/100) (b),

CNTs/MC–S (10/3/100) (c) and CNTs/MC–Y (0/3/100) (d)

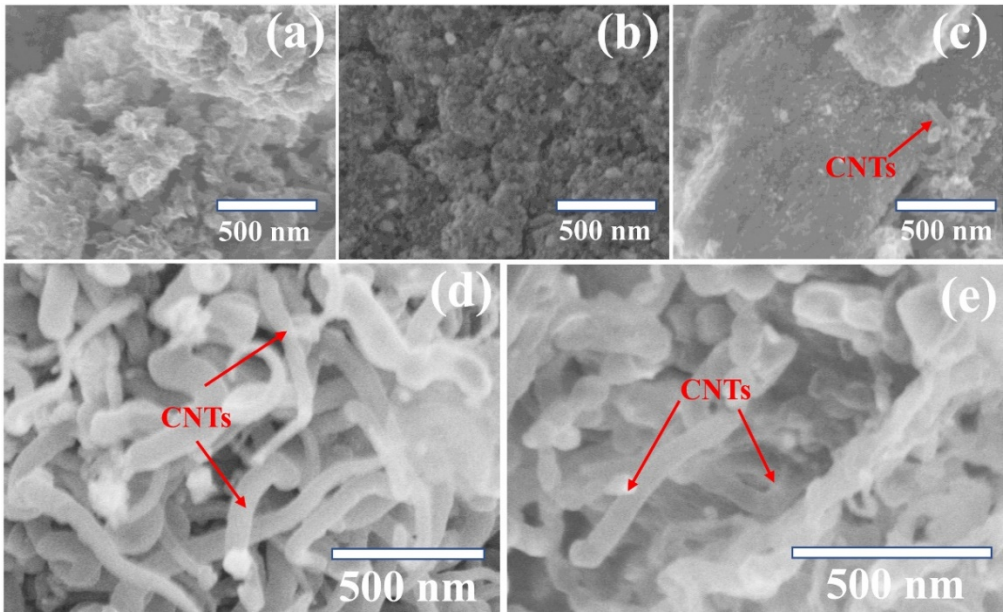

Fig. S6 SEM images of CNTs/MC–C (10/0/100) (a), CNTs/MC–G (10/1.5/100) (b), CNTs/MC–S (10/6/100) (c), CNTs/MC–Co (10/3/100) (d) and CNTs/MC–Ni (10/3/100) (e)

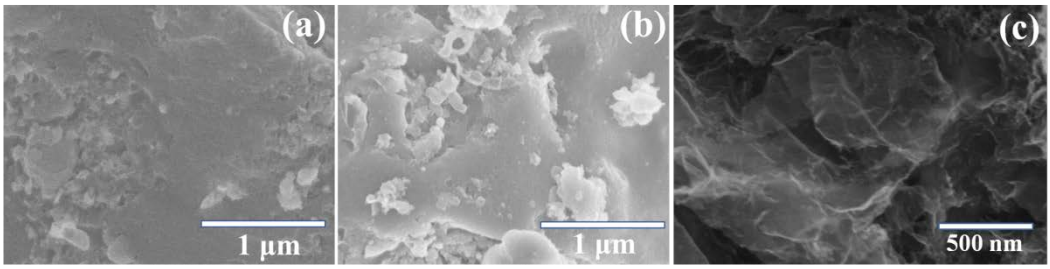

Fig. S7 SEM images of CNTs/MC–Y (10/3/0) (a), CNTs/MC–Y (10/3/10) (b) and CNTs/MC–Y (10/3/500) (c)

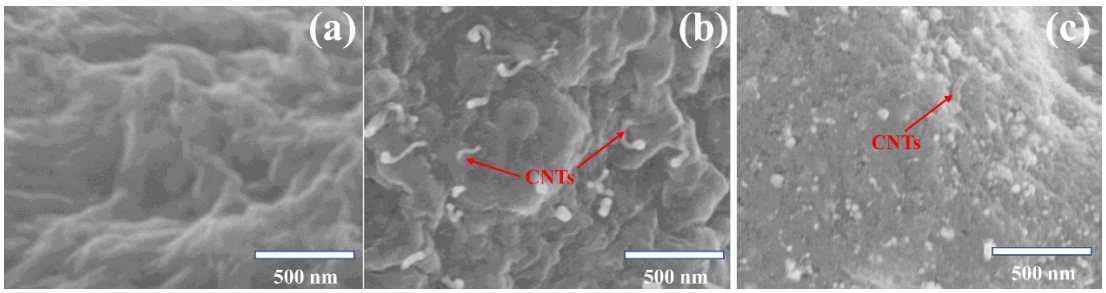

Fig. S8 SEM images of CNTs/MC–600 (10/3/100), CNTs/MC–700 (10/3/100) and CNTs/MC–900 (10/3/100)

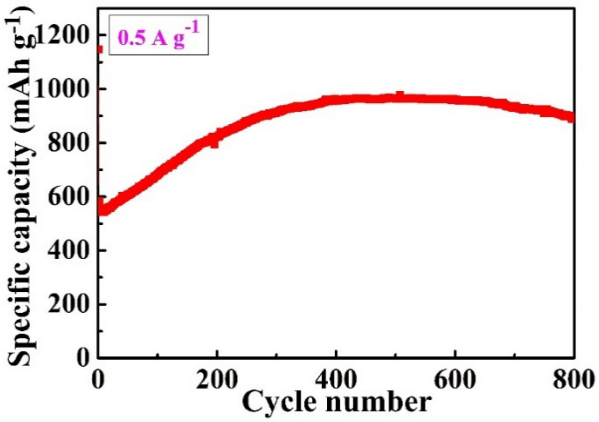

Fig. S9 Long–term cycling performance of CNTs/MC–Y (10/3/100) electrode at the current density of 0.5 A g^{-1}

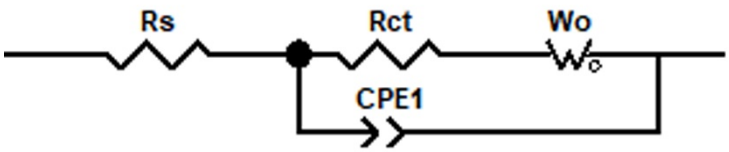

Fig. S10 Equivalent circuit model for the EIS plots

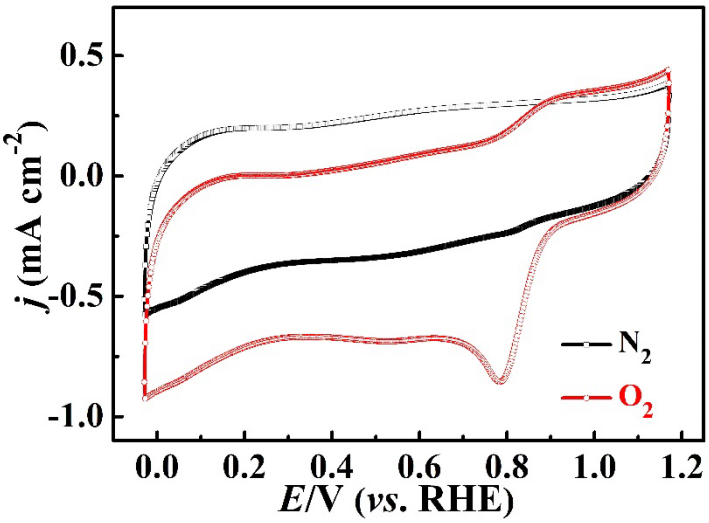

Fig. S11 CV curves on CNTs/MC–Y (10/3/100) electrode in N_2 and O_2 saturated 0.1 M KOH electrolyte

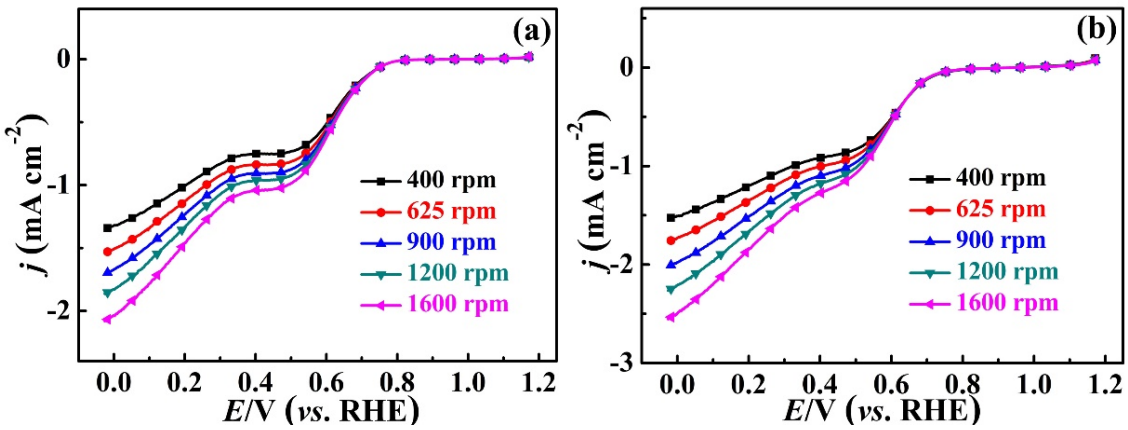

Fig. S12 LSV curves on CNTs (a) and MC (b) electrodes at different rotation speeds

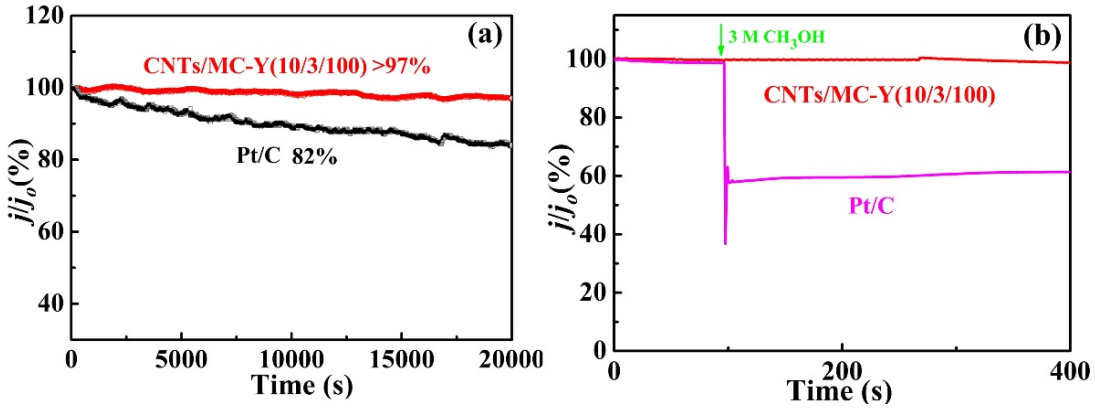

Fig. S13 (a) The relative current density *vs.* time plots on CNTs/MC–Y (10/3/100) and commercial Pt/C electrodes at 0.67 V for 20000 s in O_2 saturated 0.1 M KOH electrolyte; (b) The relative current density *vs.* time plots on CNTs/MC–Y (10/3/100) and commercial Pt/C electrodes at 0.67 V in O_2 saturated 0.1 M KOH electrolyte before and after adding 3 M methanol

Table S1 The specific BET result of different samples

Sample	Specific surface area	Pore volume
CNTs/MC–Y (10/3/100)	225.5 m^2 g^{-1}	0.62 cm^3 g^{-1}
MC	58.6 m^2 g^{-1}	0.0036 cm^3 g^{-1}
CNTs	83.1 m^2 g^{-1}	0.013 cm^3 g^{-1}

Table S2 Comparison of the ORR performance of previously reported biomass–derived carbon catalysts with that of our work

Biomass precursor	Derived catalyst	E_{onset}/V	$E_{1/2}$/V	Electrolyte	References
Yeast	CNTs/MC–Y (10/3/100)	1.01	0.81	0.1 M KOH	This work
Seaweed	Ni/NiO/$NiCo_2O_4$/ N–CNT–As	–	0.74	0.1 M KOH	Journal Material Chemistry A, 2016,4, 6376–6384
Reed	Si–Fe20/N/C–1_2	0.91	0.79	0.1 M KOH	Applied Catalysis B: Environmental, 2018, 5, 85–93
Soybean shells	NPCNS–900	0.98	–	0.1 M KOH	Physical Chemistry Chemical Physics, 2016, 18, 10392–10399.
Pine needles	PN–900	0.96	0.72	0.1 M KOH	Journal of Applied Electrochemistry, 2020, 50, 1257–1267
Dandelion seed	HHPT–900	0.83	–	0.1 M KOH	Journal of Electroanalytical Chemistry, 2019, 15, 113230
Water hyacinth	WHC–700	0.98	–	0.1 M KOH	Nanoscale, 2015, 7, 6136–6142
Silk/Chitosan	Ca@NP_6C_4	.0.94	0.76	0.1 M KOH	Journal of Alloys and Compounds, 2021, 25, 160726
Walnut shell	FeCr–N–C	0.88	0.73	0.1 M KOH	International Journal of Hydrogen Energy, 2022, DOI: 10.1016/j.ijhydene.2022.07.266